

Supplementary Information

Direct Writing of Metal Nanostructures with Focused Helium Ion Beams

Vladimir Bruevich *, Leila Kasaei *, Leonard C. Feldman and Vitaly Podzorov *

Department of Physics and Astronomy, Rutgers University, Piscataway, NJ 08854, USA;
l.c.feldman@rutgers.edu

* Correspondence: bruevich@physics.rutgers.edu (V.B.); leila.kasaei@rutgers.edu (L.K.);
podzorov@physics.rutgers.edu (V.P.)

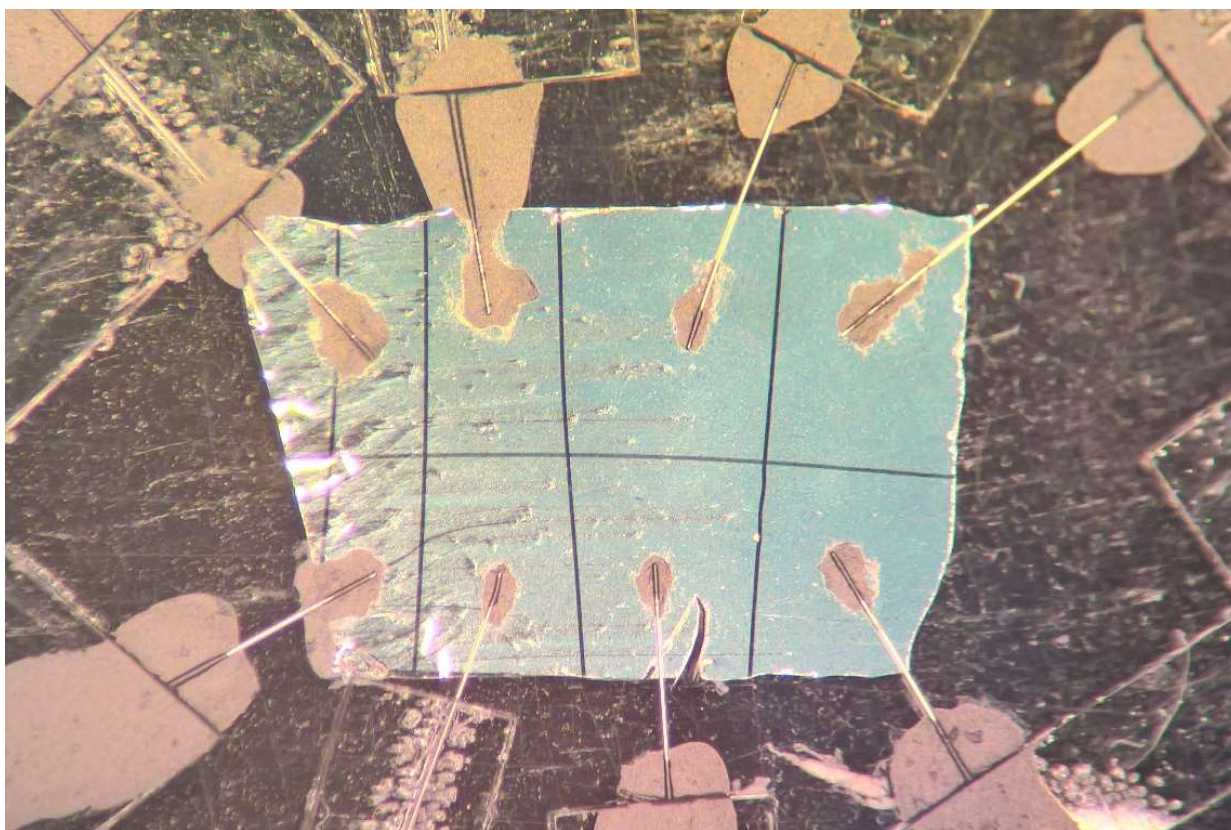


Figure S1. An example of a device layout for resistance measurements of ultra-thin metal films (an optical microphotograph). The device consists of multiple thick metal contact pads (faint blueish rectangles) with 25- μm gaps (the channels) between them, evaporated on a substrate (here, a parylene-N coated glass). Ultra-thin (typically ~ 3 nm) gold or silver films are then evaporated atop these channels (cannot be seen in this image) and can then be locally patterned with a focused ion beam of a helium-ion microscope (HIM), creating conducting micro- or nano-scale lines bridging the macroscopic contact pads (Fig. 2 of the main text). The excessive metal film around the devices is removed together with parylene-N using a sharp knife or a razor. The contact pads are wired to an external measuring circuitry with 25- μm thick silver wires attached to the pads with a graphite paint (an aqueous suspension of colloidal graphite). The typical width of the contact pads in such structures is 1 mm.

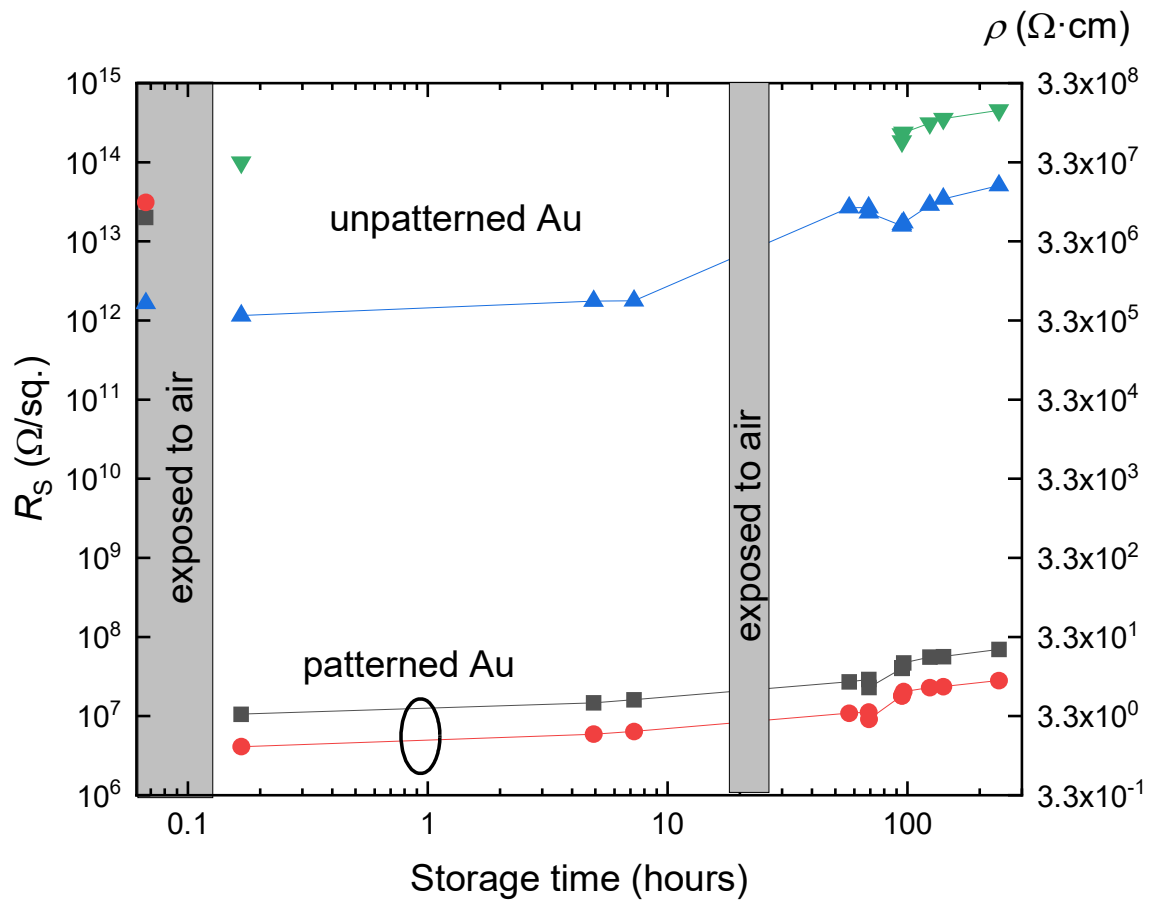


Figure S2. Monitoring the long-term resistive drift of ultrathin metal films. The sheet resistance (left axis) and the nominal bulk resistivity (right axis) of an ultra-thin (nominal thickness ~ 3.3 nm) gold film evaporated on a parylene-N substrate are shown as a function of time. Unpatterned (as-evaporated) and HIM-patterned gold films were measured. The patterning was performed with a 30 keV focused He^+ -ion beam of the HIM. The films were exposed to air twice during this measurement, with the rest of the time spent either in high vacuum or in an atmosphere of ultra-high-purity Ar gas. The gradual degradation of the film's conductivity is associated with the so-called Ostwald ripening of metal nanoparticles and their interaction with the atmosphere (see main text). Patterning with the HIM's focused ion beam reduces the rate of such degradation.

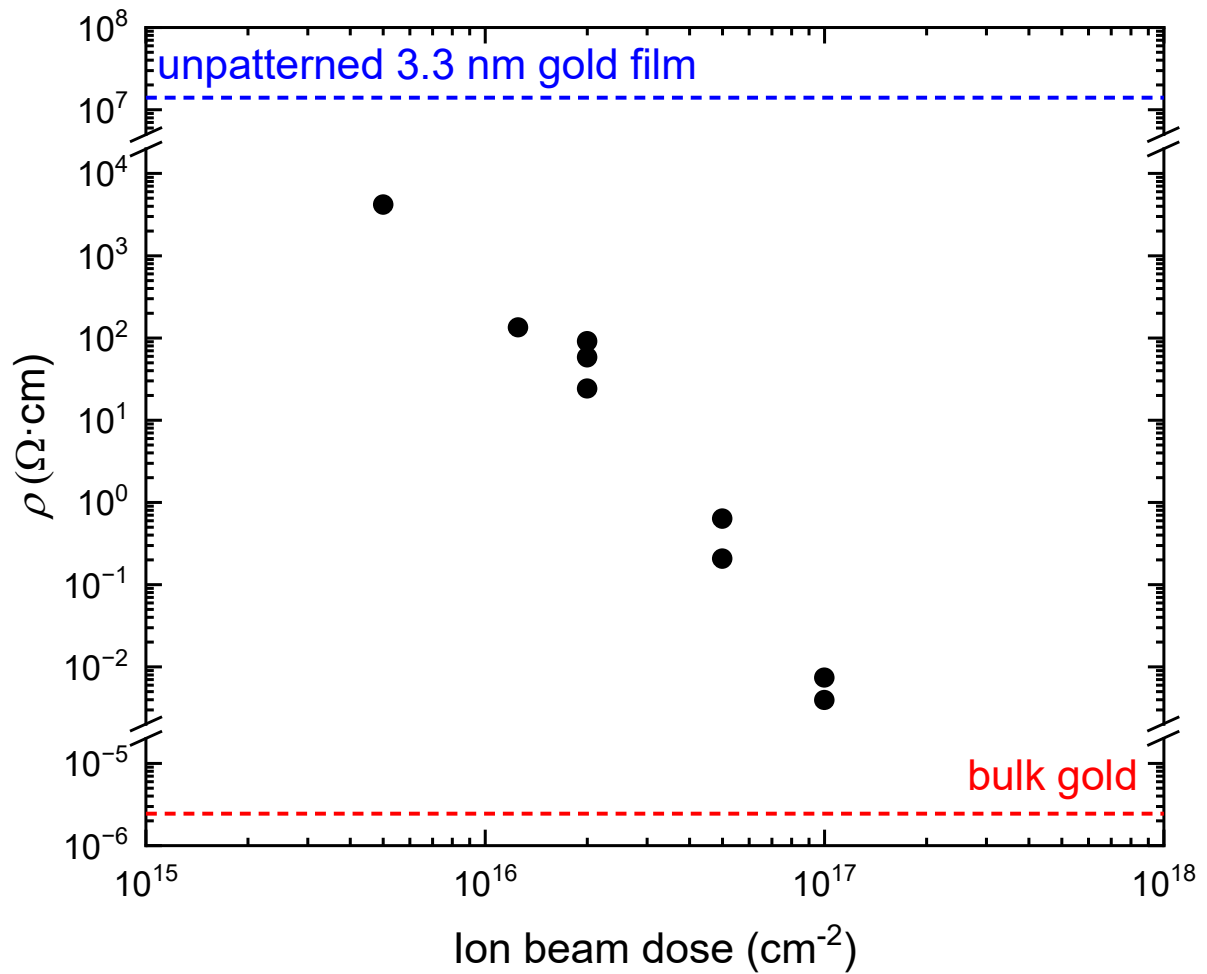


Figure S3. Experimental evaluation of the nominal 3D resistivity of HIM-patterned metallic films. The nominal resistivity ρ is calculated using the measured sheet resistance R_S (see Fig. 3 of the main text) of conducting stripes patterned with HIM in an ultrathin, insulating seed layer of gold. Ultra-thin gold of a nominal thickness $d = 3.0 \pm 0.3$ nm was evaporated on parylene-N surface. The plot shows $\rho \equiv R_S \cdot d$ as a function of the He⁺-ion beam dose. As a reference, the blue and red dashed lines show the nominal ρ of the unpatterned seed film and the tabulated ρ of the bulk solid gold ($2.44 \times 10^{-6} \Omega \cdot \text{cm}$), respectively.

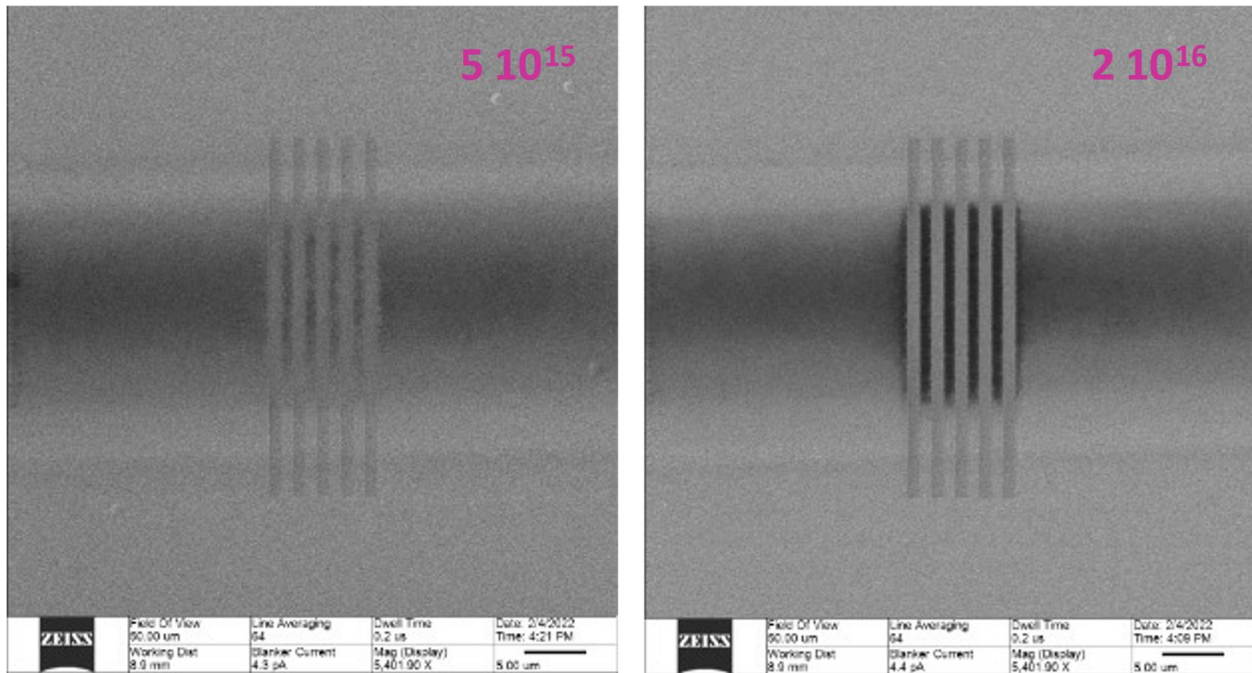


Figure S4. Examples of ultrathin gold films patterned with a focused ion beam of a helium ion microscope (HIM). The images are secondary-electron images collected with the HIM. The conducting stripes were patterned by direct writing with the focused He^+ -ion beam on a pre-evaporated ultrathin (nominal thickness of ~ 3 nm) insulating gold film on a parylene-N substrate. The results for two ion-beam doses, 5×10^{15} and 2×10^{16} cm^{-2} , are shown on the left and right panels, respectively. The scale bar is $5 \mu\text{m}$ in both cases.

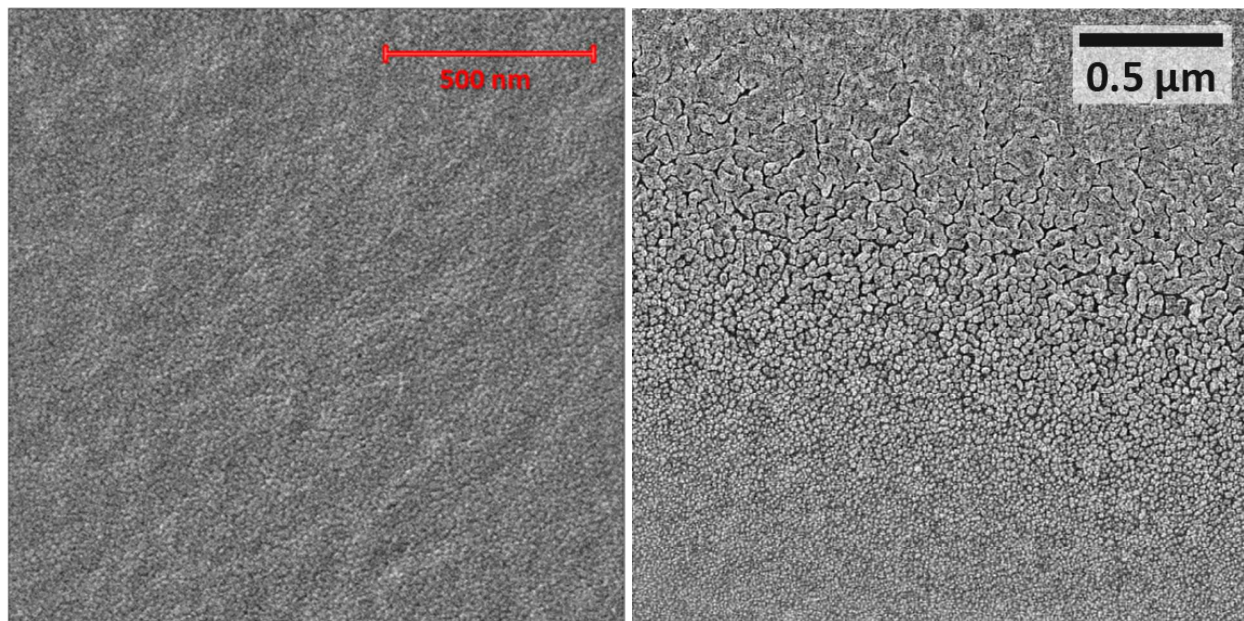


Figure S5. The secondary-electron HIM images of thin metal films. Left panel: an ultrathin (~ 3.0 nm-thick) and almost completely insulating (R_S of tens of $\text{T}\Omega/\text{sq.}$) gold film evaporated on a parylene-N surface. A uniform layer of gold nanoparticles can be discerned. Right panel: a transition region between a continuous, well-conducting, 30 nm-thick silver film (top of the image) and a masked area lacking the metal (below the bottom of the image). This spot of the sample, chosen near the edge of a masked film, features a gradient in the thickness of silver film in the vertical direction, showing the region in the middle of the panel, where a dense layer of disconnected silver nanoclusters is formed.

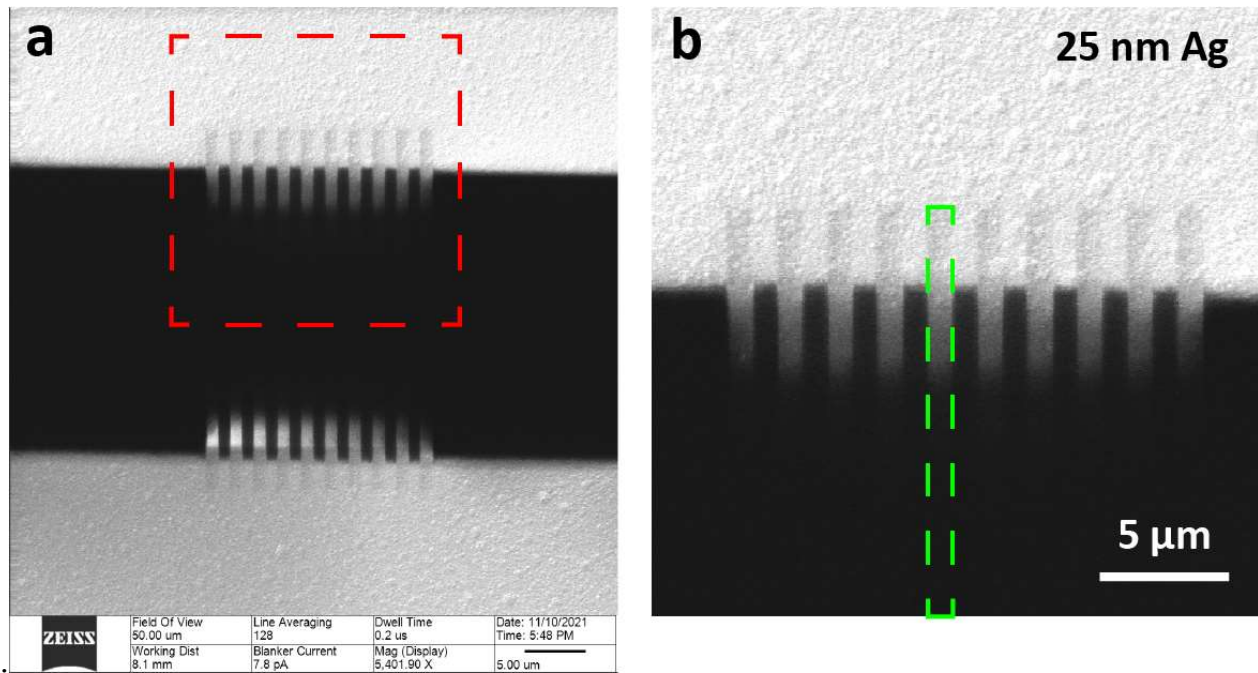


Figure S6. The secondary-electron images of HIM-patterned edges of thick silver contacts. (a) A series of parallel 1 μm wide lines patterned between a pair of 25 nm-thick, continuous silver contacts. Ag was pre-evaporated on parylene-N surface through a wire shadow mask, resulting in the contact pads separated by a 25 μm -long gap (the dark region). The red box indicates the region of the image reproduced in panel b. (b) A magnified image of a patterned region near the edge of a thick silver contact, showing the effect of HIM patterning on the image's contrast in the case of a thick metal film. The green box outlines one of the patterned stripes. The HIM patterning on thick and continuous metal films apparently has an *inverted* secondary-electron contrast in comparison with similar patterning of ultra-thin, sub-conducting films (i.e., the patterned regions here are slightly darker than the unpatterned ones). A reduced brightness is likely associated with a hydrocarbon buildup at the surface commonly occurring under focused ion beams (see main text). In contrast, a similar patterning performed on a non-conducting, ultra-thin metal film (in a zone corresponding to the "shadow" region between the contact pads) shows an increased brightness, which is associated with the modification of the sub-conductive layer of silver nanoparticles that always form under a non-contact shadow mask during the thermal evaporation of metals in high vacuum.